Participation of the S4 voltage sensor in the Mg^{2+}-dependent activation of large conductance (BK) K^+ channels

Lei Hu*†, Jingyi Shi*†, Zhongming Ma‡, Gayathri Krishnamoorthy*, Fred Sieling*, Guangping Zhang‡, Frank T. Horrigan‡, and Jianmin Cui*§

*Cardiac Bioelectricity Research and Training Center and Department of Biomedical Engineering, Case Western Reserve University, Cleveland, OH 44106; and ‡Department of Physiology, University of Pennsylvania School of Medicine, Philadelphia, PA 19104

Communicated by Clay M. Armstrong, University of Pennsylvania School of Medicine, Philadelphia, PA, July 9, 2003 (received for review April 11, 2003)

The S4 transmembrane segment is the primary voltage sensor in voltage-dependent ion channels. Its movement in response to changes in membrane potential leads to the opening of the activation gate, which is formed by a separate structural component, the S6 segment. Here we show in voltage-, Ca^{2+}-, and Mg^{2+}-dependent, large conductance K^+ channels that the S4 segment participates not only in voltage- but also Mg^{2+}-dependent activation. Mutations in S4 and the S4-S5 linker alter voltage-dependent activation and have little or no effect on activation by micromolar Ca^{2+}. However, a subset of these mutations in the C-terminal half of S4 and in the S4-S5 linker either reduce or abolish the Mg^{2+} sensitivity of channel gating. Cysteine residues substituted into positions R210 and R213, marking the boundary between S4 mutations that alter Mg^{2+} sensitivity and those that do not, are accessible to a modifying reagent [sodium (2-sulfonatoethyl)methane-thiosulfonate] (MTSES) from the extracellular and intracellular side of the membrane, respectively, at −80 mV. This implies that interactions between S4 and a cytoplasmic domain may be involved in Mg^{2+}-dependent activation. These results indicate that the voltage sensor is critical for Mg^{2+}-dependent activation and the coupling between the voltage sensor and channel gate is a converging point for voltage- and Mg^{2+}-dependent activation pathways.

Voltage-dependent ion channels generate action potentials by which nerve, heart, and muscle cells convey information of commands and stimuli (1). The voltage dependence of these channels derives from the movement of a voltage sensor, primarily the charged S4 transmembrane segment, in response to changes in the membrane potential (2–5). Such movement triggers the opening of the S6 activation gate (6–8). Recently, Jiang *et al*. (9, 10) demonstrated that the S4 and S3b transmembrane segments form a helix–turn–helix structure called the "voltage-sensor paddle" that moves across the membrane from inside to outside in response to depolarization and opens the channel.

The large conductance, voltage-, Ca^{2+}-, and Mg^{2+}-dependent K^+ (BK) channel encoded by the *slo1* gene (11) is activated by membrane depolarization and shares a similar overall transmembrane topology with voltage-dependent K^+, Na^+, and Ca^{2+} channels (1, 9, 12). The S4 transmembrane segment of BK channels contains positively charged amino acids that are conserved among voltage-dependent channels (Fig. 1 *A* and *B*), some of which serve as the gating charge for voltage-dependent activation of BK channels (13, 14). Intracellular Ca^{2+} and Mg^{2+} also activate BK channels (15–19). Mg^{2+} activates the channel by binding to low-affinity metal-binding sites that are distinct from the high-affinity sites for Ca^{2+}-dependent activation (18, 19), and the Mg^{2+}-binding site is located in the intracellular RCK domain of the channel protein (20–22). The RCK domain adopts a Rossmann fold structure and is conserved among BK channels as well as various prokaryotic K^+ channels where it regulates K^+ conductance (20, 23). The binding of Mg^{2+} in the intracellular RCK domain opens the activation gate by an allosteric mechanism (18, 19).

Here we report that mutations in S4 and the S4-S5 linker not only affect voltage dependence but also reduce or abolish the Mg^{2+} sensitivity of channel activation. The residues whose mutation affects Mg^{2+} sensitivity are located at the intracellular side of the membrane when the channel is closed, suggesting that the interaction between the intracellular RCK domain and the voltage-sensor paddle as well as the S4-S5 linker (9, 10) is critical for Mg^{2+}-dependent activation. Thus Mg^{2+}- and voltage-dependent activation are both under the influence of the voltage sensor, and coupling between S4 and the activation gate is likely to serve as a common feature of these two pathways.

Methods

Mutagenesis and Expression. All channel constructs were made from the mbr5 clone of the mouse slo1 BK channel (mslo1) (24) by using PCR (21) with *Pfu* polymerase (Stratagene). The PCR-amplified regions of all mutants were verified by sequencing. RNA was transcribed *in vitro* with T3 polymerase (Ambion, Austin, TX). We injected 0.05–50 ng of RNA into each *Xenopus laevis* oocyte 2–6 days before recording.

Electrophysiology. Macroscopic currents were recorded from excised patches in the inside-out or outside-out configuration by using an Axopatch 200-B patch-clamp amplifier (Axon Instruments, Foster City, CA) and PULSE acquisition software (HEKA Electronics, Lambrecht/Pfalz, Germany). Records were low-pass-filtered at 10 kHz with the amplifier's built-in four-pole Bessel filter and digitized at 20-μs intervals. The external solution contained 140 mM K-methanesulfonic acid, 20 mM Hepes, 2 mM KCl, and 2 mM $MgCl_2$, pH 7.20. The basal internal solution contained 140 mM K-methanesulfonic acid, 20 mM Hepes, 2 mM KCl, and 1 mM EGTA, pH 7.20. The "0 $[Ca^{2+}]_i$" solution was the same as the basal internal solution except that it contained 5 mM EGTA having a free $[Ca^{2+}]_i$ of ≈0.5 nM, which is too low to affect mslo1 channel activation (25). $CaCl_2$ and $MgCl_2$ were added to internal solutions to give the appropriate free $[Ca^{2+}]_i$ and $[Mg^{2+}]_i$ (18). The final free $[Ca^{2+}]_i$ was measured by using a Ca^{2+}-sensitive electrode (Orion, Boston). All recordings were performed at room temperature (22–24°C). A 500 mM stock solution of sodium (2-sulfonatoethyl)methanethiosulfonate (MTSES, Toronto Research Chemicals, Downsview, ON, Canada) dissolved in DMSO (Sigma) was made, stored at −20°C, and diluted in the external or internal solution

Abbreviations: BK, large conductance, voltage-, Ca^{2+}-, and Mg^{2+}-dependent K^+; mslo1, mouse slo1 BK channel; MTSES, sodium (2-sulfonatoethyl)methane-thiosulfonate; *G–V*, conductance-voltage; KvAP, a voltage-dependent K^+ channel of *Aeropyrum pernix*.

†L.H. and J.S. contributed equally to this work.

§To whom correspondence should be addressed at: Department of Biomedical Engineering, Case Western Reserve University, 522 Wickenden Building, 10900 Euclid Avenue, Cleveland, OH 44106-7207. E-mail: jxc93@cwru.edu.

 www.pnas.org/cgi/doi/10.1073/pnas.1834300100

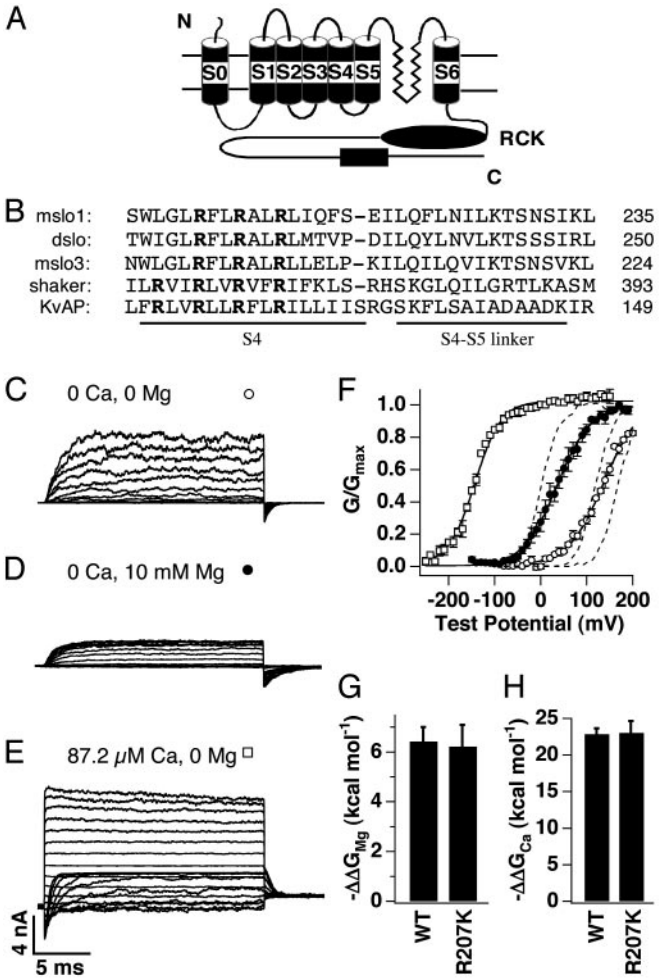

Fig. 1. Results of mutation R207K. (*A*) Diagram of the slo polypeptide. S0–S6, transmembrane segments; RCK, RCK domain (20). (*B*) Sequence alignment (9) of the S4 segment (underlined) and S4-S5 linker region from mslo1 (24), dslo (11), and mslo3 (33) BK channels, Shaker (34), and KvAP (9) K^+ channels. Numbers indicate the position of the right-most residues in the primary sequence of their respective proteins. Boldface type indicates conserved positively charged amino acids in S4. (*C–E*) Currents of R207K channels recorded at indicated $[Mg^{2+}]_i$ and $[Ca^{2+}]_i$. Testing potentials were −150 to +190 mV (*C* and *D*) or −250 to +150 mV (*E*) with 20-mV increments. The holding and repolarizing potentials were −80 and −50 mV. (*F*) Mean *G–V* relations of R207K (symbols) and WT mslo1 (dashed lines) channels at $[Mg^{2+}]_i$ and $[Ca^{2+}]_i$ as indicated in *C–E*. *G–V* relations of R207K channels are fitted with the Boltzmann relation (solid lines, see *Methods*). (*G* and *H*) Free energy provided by Mg^{2+} (*G*) or Ca^{2+} (*H*) binding in activating channels (see *Methods*) when $[Mg^{2+}]_i$ increased from 0 to 10 mM at 0 $[Ca^{2+}]_i$ (*G*) or when $[Ca^{2+}]_i$ increased from 0 to 87.2 μM at 0 $[Mg^{2+}]_i$ (*H*).

immediately before perfusion (SF-77B Perfusion Fast-Step, Warner, Hamden, CT) to achieve a final concentration of 500 μM.

Analysis. Relative conductance was determined by measuring tail current amplitudes at −50 mV. Conductance–voltage (*G–V*) relations were fitted with the Boltzmann distribution

$$G/G_{max} = 1/[1 + \exp(\Delta G_{Act}/kT)], \quad [1]$$

where k is Boltzmann's constant, T is absolute temperature, and ΔG_{Act} is the free-energy change of channel opening. ΔG_{Act} is the sum of energy increases provided by voltage ($\Delta G_V = -zeV$, where e is the elementary charge and z is the number of equivalent charges), Ca^{2+} and Mg^{2+} binding (ΔG_{Ca}, ΔG_{Mg}), and that in the absence of Ca^{2+} and Mg^{2+} at 0 mV (ΔG_0) (14, 18, 21),

$$\Delta G_{Act} = \Delta G_V + \Delta G_{Ca} + \Delta G_{Mg} + \Delta G_0. \quad [2]$$

The change in Ca^{2+}- or Mg^{2+}-binding contribution to ΔG_{Act} as a result of a $[Ca^{2+}]_i$ or $[Mg^{2+}]_i$ increase, $\Delta\Delta G_{Ca}$ or $\Delta\Delta G_{Mg}$, was then calculated based on the shift and change in shape of the *G–V* relation between two specified values of $[Ca^{2+}]_i$ or $[Mg^{2+}]_i$,

$$\Delta\Delta G_{Ca} = -\Delta(zeV_{1/2}) \text{ or } \Delta\Delta G_{Mg} = -\Delta(zeV_{1/2}), \quad [3]$$

where $V_{1/2}$ is the voltage at half-maximum of the *G–V* relation (Figs. 1 *G* and *H* and 2 *E* and *F*). In Fig. 3*C*, $\Delta\Delta G_{Mg}$ of mutant channels was measured between 0 and 10 mM $[Mg^{2+}]_i$ in a $[Ca^{2+}]_i$ at which we were able to measure complete *G–V* relations [either 0 or high Ca^{2+} (87.2 or 95.1 μM)] (18, 21) and then divided by the mean $\Delta\Delta G_{Mg}$ of the WT mslo1 under the same condition. In Fig. 3*D*, $\Delta\Delta G_{Ca}$ of mutant channels was measured at 0 $[Mg^{2+}]_i$ and between two $[Ca^{2+}]_i$ values (14, 18, 21) at which we were able to measure a complete *G–V* relation and then divided by the mean $\Delta\Delta G_{Ca}$ of the WT mslo1 under the same condition. The $[Ca^{2+}]_i$ values for R207K, R207Q, R228Q, N231A, and S232A were 0 and 87.2 μM; for R201Q, Q216R, E219Q, and Q222R, 2.9 and 87.2 μM; for L204A, L204H, and L224R, 11.8 and 95.1 μM; for R213Q and double mutation of E219R/Q222R, were 10.5 and 87.2 μM; and for R210Q and R210N, 0 and 2.9 μM.

The error bars in all figures show standard error of means with 4–12 measurements.

Results and Discussion

The activation of BK channels by voltage, intracellular Mg^{2+}, and intracellular Ca^{2+} is initiated by three distinct structural components (S4, the low- and high-affinity metal-binding sites). Mutation of certain residues can perturb activation by one stimulus without affecting others. For example, mutation of certain residues in the RCK domain changes either Mg^{2+} or Ca^{2+} sensitivity but not both (21), whereas mutation of several residues in S4 alters voltage-dependent activation but does not affect Ca^{2+} sensitivity of mslo1 channels (14). Fig. 1 *C–H* shows an example of such a mutation in the S4 voltage sensor of mslo1 (R207K) in which arginine at position 207 was mutated to lysine. In 0 $[Mg^{2+}]_i$ and 0 $[Ca^{2+}]_i$ the *G–V* relation of R207K channels is shifted to a less positive voltage range and the slope is more shallow than the WT mslo1 (Fig. 1*F*). Because under this condition the channel is activated by only voltage (25), the changes in *G–V* relation indicate that the mutation affects voltage-dependent activation. On the other hand, the free energy provided by Mg^{2+} or Ca^{2+} binding in activating R207K remains the same as in activating the WT mslo1 channel (Fig. 1 *G* and *H*). Thus, the structural components and their related intramolecular interactions that are affected by the R207K mutation may participate in the voltage-dependent activation pathway but appear unimportant for Mg^{2+}- or Ca^{2+}-dependent activation pathways. These results suggest that voltage, Mg^{2+}, and Ca^{2+} activate the channel through distinct intramolecular pathways by affecting different sets of local conformational changes that eventually lead to channel opening. Such a mechanism is also supported by various functional studies (18, 19, 26, 27).

Although the conformational changes induced by voltage, Mg^{2+}, and Ca^{2+} are distinct to some extent, they all lead eventually to the opening of the activation gate. Therefore, the individual intramolecular activation pathways should converge, i.e., some structural components should be common to several activation pathways. The perturbation of such common structural components by mutation should affect the activation by two

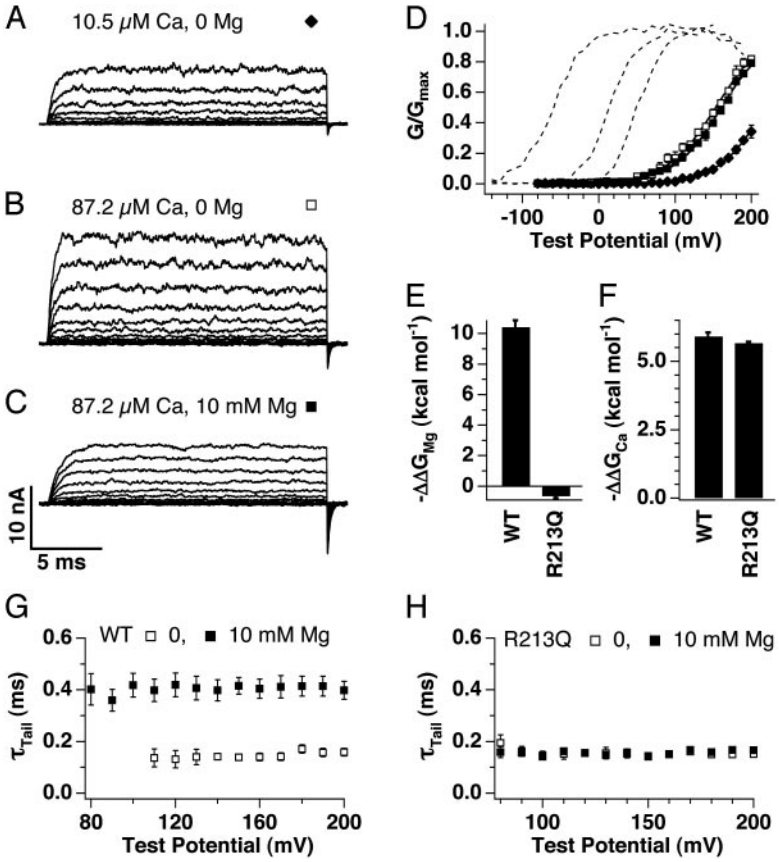

Fig. 2. Results of mutation R213Q. (*A–C*) Currents of R213Q channels recorded at indicated $[Mg^{2+}]_i$ and $[Ca^{2+}]_i$. Testing potentials were −80 to +200 mV with 20-mV increments. The holding and repolarizing potentials were −80 and −50 mV. (*D*) Mean *G–V* relations of R213Q (symbols) and WT mslo1 (dashed lines) channels at $[Mg^{2+}]_i$ and $[Ca^{2+}]_i$ as indicated in *A–C*. *G–V* relations of R213Q channels are fitted with the Boltzmann relation (solid lines). (*E* and *F*) Free energy provided by Mg^{2+} (*E*) or Ca^{2+} (*F*) binding in activating channels when $[Mg^{2+}]_i$ increased from 0 to 10 mM at 87.2 μM $[Ca^{2+}]_i$ (*E*) or when $[Ca^{2+}]_i$ increased from 10.5 to 87.2 μM at 0 $[Mg^{2+}]_i$ (*F*). (*G* and *H*) Time constant of tail currents at −50 mV as the voltage stepped down from a series of test potentials at 0 or 10 mM $[Mg^{2+}]_i$ and 87.2 μM $[Ca^{2+}]_i$ for WT mslo1 (*G*) and R213Q (*H*) channels.

or all three stimuli. Surprisingly, one example of such a mutation is another S4 mutation (R213Q) that not only alters voltage dependence but also abolishes Mg^{2+}-dependent activation (Fig. 2). Consistent with a previous report (14), this mutation shifts the *G–V* relation to a very positive voltage range and reduces its slope (Fig. 2*D*). However, Ca^{2+} sensitivity is not affected (Fig. 2*F*), suggesting that the high-affinity binding site and Ca^{2+}-dependent activation pathway are not altered. Because R213 may serve as a gating charge (ref. 13 and Fig. 4), the effects of mutation on voltage dependence are not surprising. However, the *G–V* relation for R213Q is the same in either the absence or presence of 10 mM $[Mg^{2+}]_i$ (Fig. 2*D*), indicating that the channel also loses its Mg^{2+} sensitivity. For the WT mslo1 channel (Fig. 2*G*) and mutant channels that are sensitive to Mg^{2+} (Figs. 1 *C* and *D* and 2 *E* and *F*) the time course of deactivation at −50 mV in the presence of Mg^{2+} is slower than in the absence of Mg^{2+}. In contrast, the deactivation of R213Q is unaffected by 10 mM $[Mg^{2+}]_i$ (Fig. 2*H*), further supporting that Mg^{2+} sensitivity is lost as a result of the mutation. Two lines of evidence suggest that the R213Q mutation abolishes Mg^{2+} sensitivity by affecting the intramolecular interaction between R213 and the local structure immediately surrounding it: (*i*) Ca^{2+} sensitivity of the channel is not affected by the mutation (Fig. 2*F*), suggesting that the mutation does not affect channel gating by causing a global perturbation of channel structure, and (*ii*) mutations of R210, only three residues away from R213, do not affect Mg^{2+} sensitivity, although they alter both voltage and Ca^{2+} sensitivity (Fig. 3 *A–D*, for R210N and R210Q, and *E–J*, for R210N), suggesting that the structural components affected by R213 and R210 mutations do not overlap. The total loss of Mg^{2+} sensitivity that results from disruption of such a local structure indicates that the interaction between R213 and its adjacent structure is part of the Mg^{2+}-dependent activation pathway and could contribute to the allosteric mechanism that couples Mg^{2+} binding to channel opening (18, 19).

Fig. 3 *A–D* shows the results of systematic point mutations throughout the S4 segment and the S4–S5 linker. As expected, many the mutations in S4 change the voltage dependence of channel activation by shifting the *G–V* relation in 0 $[Mg^{2+}]_i$ and 0 $[Ca^{2+}]_i$ to different voltage ranges (Fig. 3*A*) and/or altering the slope of the *G–V* relation (Fig. 3*B*). The change in voltage dependence is most prominent when the residues between positions 207 and 224 are mutated (except for E219Q, Fig. 3 *A* and *B*). However, the effects of these mutations on Mg^{2+} sensitivity exhibit a different pattern with regard to the position of mutated residues (Fig. 3*C*). The mutations in the C-terminal half of S4 and the N-terminal part of the S4-S5 linker (R213–L224) all reduce Mg^{2+} sensitivity, whereas those in the rest of S4 or S4-S5 linker that flank this region (R201–N210 and K228–S232) do not (Fig. 3*C*). These results suggest that interactions between residues in the region spanning the C-terminal half of S4 and the N-terminal part of the S4-S5 linker with their adjacent structures are important in transmitting the energy of Mg^{2+} binding to the opening of the channel gate. Consistent with such

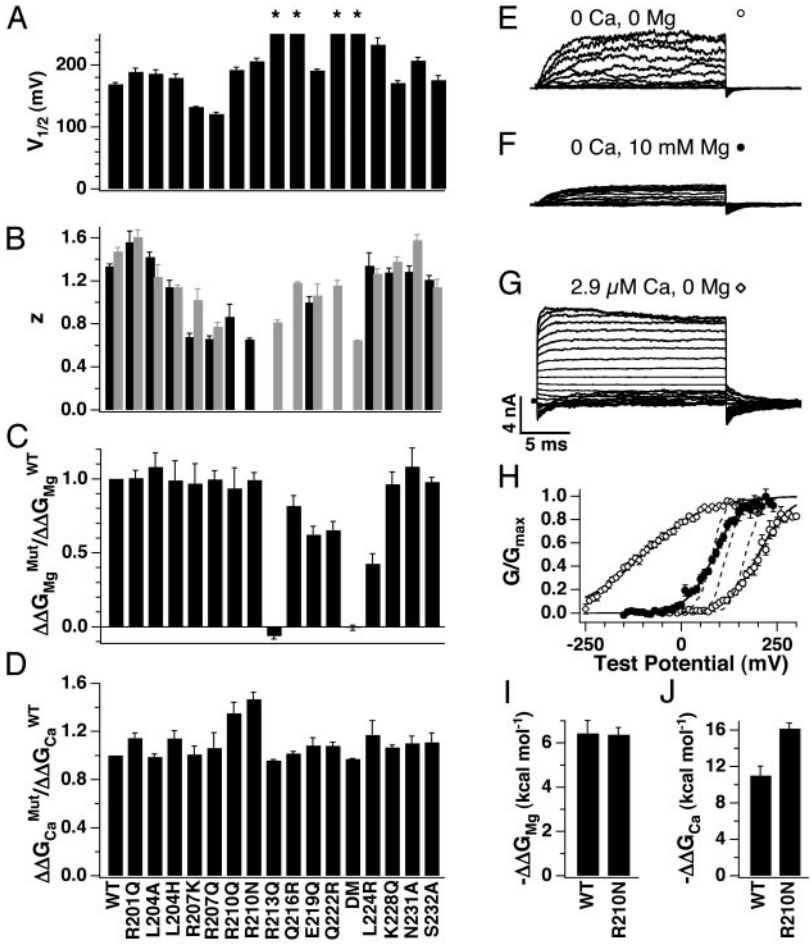

Fig. 3. Summary of mutational results and results of mutation R210N. (*A–D*) $V_{1/2}$ of *G–V* relations (see *Methods*) measured at 0 $[Mg^{2+}]_i$ and $[Ca^{2+}]_i$ (*A*), *z* (see *Methods*) at 0 (dark bars) and 87.2 or 95.1 μM (gray bars) $[Ca^{2+}]_i$ and 0 $[Mg^{2+}]_i$ (*B*), normalized free energy provided by Mg^{2+} binding (*C*), and normalized free energy provided by Ca^{2+} binding (*D*) of WT mslo1 and mutant channels. DM, double mutation of E219R/Q222R. The *G–V* relation of R213Q, Q216R, Q222R, and DM was shifted to very high voltage ranges such that little channel activity could be observed at 0 $[Mg^{2+}]_i$ and $[Ca^{2+}]_i$. Thus, $V_{1/2}$ of these mutant channels in *A* is estimated to be more than +250 mV and is indicated by ∗. In *B*, for some mutant channels, *z* could not be measured accurately either at 0 or 87.2∼95.1 μM $[Ca^{2+}]_i$ due to extreme voltage ranges of their *G–V* relation. (*E–G*) Currents of R210N channels recorded at indicated $[Mg^{2+}]_i$ and $[Ca^{2+}]_i$. Testing potentials were −100 to +300 mV (*E*), −150 to +250 mV (*F*), or −250 to +190 mV (*G*) with 20-mV increments. The holding and repolarizing potentials were −80 and −50 mV. (*H*) Mean *G–V* relations of R210N (symbols) and WT mslo1 (dashed lines) channels at $[Mg^{2+}]_i$ and $[Ca^{2+}]_i$ as indicated in *E–G*. *G–V* relations of R210N channels are fitted with the Boltzmann relation (solid lines). (*I* and *J*) Free energy provided by Mg^{2+} (*I*) or Ca^{2+} (*J*) binding in activating channels when $[Mg^{2+}]_i$ increased from 0 to 10 mM at 0 $[Ca^{2+}]_i$ (*I*) or when $[Ca^{2+}]_i$ increased from 0 to 2.9 μM at 0 $[Mg^{2+}]_i$ (*J*).

a mechanism, the double mutation E219R/Q222R, similar to R213Q, completely abolishes Mg^{2+} sensitivity (Fig. 3*C*). It is conceivable that interactions involving the N-terminal half of S4 are important for Mg^{2+} sensitivity but are not disrupted by particular mutations. To test this possibility, residues L204, R207, and R210 were each replaced with two amino acids of different chemical properties. The different mutations at each of these residues alter voltage dependence (Fig. 3 *A* and *B*) but do not affect Mg^{2+} sensitivity (Fig. 3*C*). These results suggest that the N-terminal half of S4 does not participate in the Mg^{2+}-dependent activation pathway. Fig. 3*D* shows that most mutations have little effect on Ca^{2+} sensitivity except that mutations of R210 increase Ca^{2+} sensitivity significantly (also see Fig. 3 *H* and *J*), further supporting that Mg^{2+} and Ca^{2+} activate the channel through distinct pathways.

One structural feature that may distinguish the N- and C-terminal halves of the S4 segment is their membrane topology. Residues R210 and R213, marking the boundary between mutations that alter Mg^{2+} sensitivity and those that do not, have been proposed to act as gating charges (13) and therefore should lie near the membrane–solution interface. To test this hypothesis we mutated R210, R213, and Q216 individually to cysteine and studied their accessibility to the membrane-impermeable cysteine-modifying reagent MTSES from intracellular and/or extracellular solutions at −80 mV where most channels were closed (Fig. 4). The results in Fig. 4 show that each position can be modified, producing a decrease in the amplitude of currents evoked by brief (20-ms) depolarizing test pulses (Fig. 4 *A–C*) and a shift in the *G–V* relationship (Fig. 4 *D–F*). However, 210C is modified only from the extracellular solution (Fig. 4*A*), whereas 213C and 216C are only modified from the intracellular solution (Fig. 4 *B* and *C*), which suggests that the C-terminal half of S4 may differ from the N-terminal half in its availability to interact with structural domains at the cytoplasmic side that transduce Mg^{2+} binding into channel opening. It is likely that the role of such interactions in the Mg^{2+}-dependent activation pathway is to mediate the allosteric linkage through which conformational changes in the Mg^{2+}-binding site are coupled to channel opening (18, 19, 28). Thus, although S4 residues, many of which are positively charged, are unlikely to participate directly in Mg^{2+}

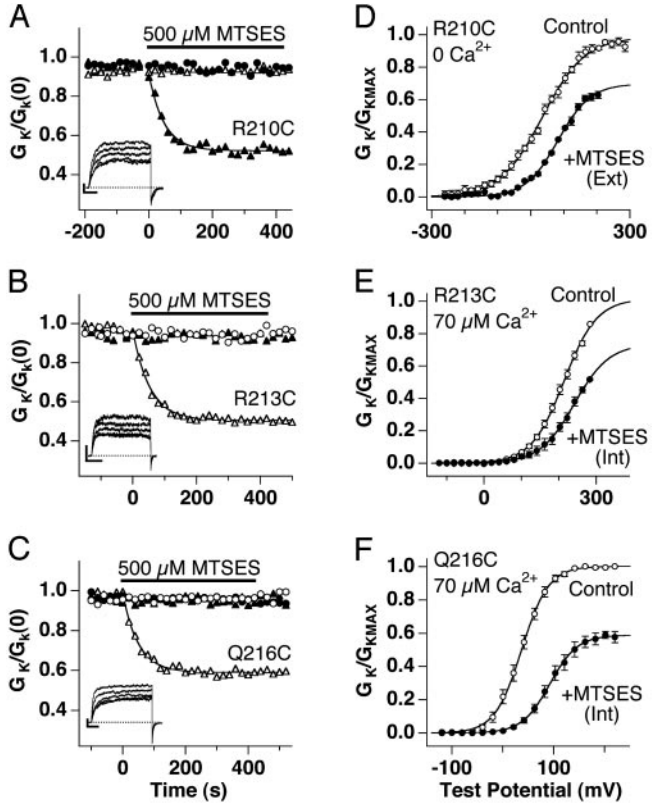

Fig. 4. Cysteine residues introduced in the N- or C-terminal half of the S4 segment are modified by MTSES from the extracellular or intracellular solution, respectively. MTSES (500 μM) was applied to excised patches in the inside-out or outside-out configuration. I_K was evoked by 20- to 30-ms test pulses to +200 mV at 5-s intervals from a holding potential of −80 mV in 0 $[Mg^{2+}]_i$. Because voltage dependence can be altered by S4 mutation and mslo1 channels contain native cysteines, each cysteine mutant (R210C, R213C, and Q216C) was compared with a control (R210N, R213Q, and WT) where the S4 cysteine was replaced by another neutral residue. Different cysteine mutants were studied under different $[Ca^{2+}]_i$ (below); however, cysteine mutant/control pairs were always studied under the same conditions. (*A–C*) G_K, determined from steady-state I_K during each test pulse, plotted for every fourth pulse, and normalized to $t = 0$, is stable preceding application of MTSES (solid bar). Modification of cysteine mutants from the intracellular (△) or extracellular (▲) solution produced an irreversible decrease in G_K to a nonzero steady state in ≈200 s. (*Insets*) These traces also show the decrease in I_K evoked by individual test pulses during modification by MTSES. (Scale bars, 2 nA and 5 ms.) Control channels were unaffected by MTSES from either intracellular (○) or extracellular (●) solution. (*A*) R210C is modified from the extracellular (0 $[Ca^{2+}]_i$) but not the intracellular (1 μM $[Ca]_i$) solution. (*B*) R213C is modified from the intracellular (70 μM $[Ca^{2+}]_i$) but not the extracellular (70 μM $[Ca^{2+}]_i$) solution. (*C*) Q216C is modified from the intracellular (70 μM $[Ca^{2+}]_i$) but not the extracellular (0 $[Ca^{2+}]_i$) solution. (*D–F*) Mean normalized G_K–V relations, determined from tail currents, for cysteine mutants before (○) and after (●) steady-state modification by MTSES show a decrease at all voltages consistent with both an increase in $V_{1/2}$ and a decrease in G_{KMAX} determined from Boltzmann fits (lines). Control G_K–V relations exhibited no significant change in either $V_{1/2}$ or G_{KMAX} (*t* test) after exposure to 500 μM MTSES for 600 s (data not shown).

binding, their mutation could result in reduced Mg^{2+} sensitivities of channel activation (Fig. 3) by decoupling the conformational changes of the activation gate from those of the Mg^{2+}-binding site.

Recently, Jiang *et al.* (9, 10) solved the crystal structure of a voltage-dependent K^+ channel cloned from *Aeropyrum pernix* (KvAP) and elucidated the voltage-dependent movements of its voltage-sensor paddle. Our results are remarkably consistent with their proposed structure and model of voltage-dependent gating. The residues in mslo1 that are important to both voltage- and Mg^{2+}-dependent activation (R213–L224) span a region, corresponding to R124–L138 in KvAP, that includes part of the S4 and S4-S5 linker helices and a flexible domain between them (9). This region is proposed to protrude from the membrane toward the intracellular side when the channel is closed (10), consistent with the idea that it may be available, in mslo1, to interact with the intracellular RCK domain where Mg^{2+} binds. It is remarkable that the residues L125 and I127 in the KvAP channel were accessible to the internal side of membrane, which marks the boundary on the S4 helix between intracellular solution and the membrane (10). The residue R126 between these two residues in KvAP corresponds to R213 in the mslo1 channel (9) that also marks the boundary between S4 mutations that alter Mg^{2+} sensitivity and those that do not (Fig. 3) as well as the boundary for S4 residues that are accessible to MTSES modification from the intracellular side of the membrane (Fig. 4). Another important feature of the proposed KvAP gating mechanism is that the S4 and S4-S5 linker helices move into the membrane after depolarization and also undergo a large change in their relative orientation that is required for coupling voltage-sensor movement to channel opening (10). Thus, conformational changes in this region are linked to multiple steps in the voltage-dependent activation pathway. It therefore seems reasonable that interactions of the RCK domain with the S4 and S4-S5 linker could be involved in transmitting the energy of Mg^{2+} binding to the opening of the channel gate by either influencing voltage-sensor movement or the coupling between voltage sensor and gate. In either case, coupling between S4 and the gate would be required to transduce Mg^{2+} binding into channel opening and therefore serves as a common feature of both voltage- and Mg^{2+}-dependent activation pathways.

It is intriguing that the coupling between Mg^{2+} binding and channel gate in the Mg^{2+}-dependent activation pathway may involve the identical structural components that couples voltage-dependent S4 movements to gate opening. Consistent with this possibility, mutations in the C-terminal half of S4 and the S4-S5 linker that reduce Mg^{2+} sensitivity also shift the G–V relation to more positive voltage ranges and reduce its slope (Figs. 2 and 3). Previous studies in the Shaker K^+ channel demonstrated that conservative mutations in the C-terminal half of S4 V369I/I372L/S376T (ILT) separate the voltage dependence of the closed-to-open transition from that of the bulk of gating charge movements (29), which may result from the disruption of the coupling between S4 movements and the opening of the activation gate. These results suggest that the C-terminal half of S4 in BK and Shaker K^+ channels may share similar functions in transmitting the energy of S4 voltage-sensor movements to channel opening.

Although the Mg^{2+}-binding site is located in the RCK domain (21, 22), our results show that the mechanism of Mg^{2+}-dependent activation in BK channels must differ from that of Ca^{2+}-dependent activation in MthK, a channel that is activated by low-affinity binding of Ca^{2+} to the intracellular RCK domains (23). MthK does not possess the S4 segment that seems critical for Mg^{2+}-dependent activation of mslo1. In addition, the Mg^{2+}- and Ca^{2+}-binding sites of BK and MthK, respectively, are located at very different positions in the RCK domain (21). Thus the proposed MthK mechanism, in which the intracellular RCK domains directly pull the inner pore helices (corresponding to S6 in BK channels) to open the channel after Ca^{2+} binding (8, 23), cannot readily be adapted to BK channels. Rather, Mg^{2+}-dependent activation of BK channels seems to be mediated by the S4 and S4-S5 linker and is likely to converge with the pathway that is used by voltage-dependent gating. It is worth noting that many other ligand-gated ion channels, although not always voltage-dependent, do possess the S4 segment including the hyperpolarization-activated cyclic nucleotide-gated channels

(HCN), cyclic nucleotide-gated channels (CNG), and small-conductance Ca^{2+}-activated K^+ channels (SK). Thus our results may have implications for ligand-dependent mechanisms in these channels.

Our results also highlight important differences between the mechanisms of Mg^{2+}- and Ca^{2+}-dependent activation in BK channels. The effects of micromolar Ca^{2+} on BK channel gating are well described by allosteric models that assume that Ca^{2+} and voltage act almost independently to promote channel opening (14, 25–27, 30–32). This separation between Ca^{2+}- and voltage-dependent pathways is supported by our observation that S4 mutations have little or no effect on Ca^{2+} sensitivity. In contrast, Mg^{2+} sensitivity is strongly affected by S4 mutation. Several allosteric models can reproduce the steady-state response of mslo1 BK channels to Mg^{2+} (18, 19). Alternative schemes that include or exclude interaction between Mg^{2+}-binding and voltage-sensor movement cannot be distinguished based on these data (19). However the response to millimolar Ca^{2+} supports the possibility that interactions between the Mg^{2+}- and voltage-dependent pathway exist (27). Millimolar Ca^{2+} and Mg^{2+} both act at the low-affinity binding site to shift the *G–V* relation (18, 19). An increase in Ca^{2+} from 100 μM to 1 mM shifts the *G–V* by approximately −30 mV but has little effect on open probability at −120 mV (27). The *G–V* shift is thought to represent action at the Mg^{2+}-binding site (18, 19). However, the lack of a response at more negative voltages is not consistent with independence of the Mg^{2+}- and voltage-dependent pathways (27). This together with our findings that S4 mutations reduce or abolish Mg^{2+} sensitivity and that these mutations also affect voltage dependence strongly support the idea that although the Mg^{2+}- and voltage-dependent activation pathways may be initiated by independent sensors, they both involve the S4 segment and the S4-S5 linker and therefore converge at a point before channel opening.

The mslo1 clone was kindly provided to us by Larry Salkoff. We thank Rick Aldrich, Carol Deutsch, Steve Baylor, and Toshinori Hoshi for critical review of the manuscript and helpful discussions. This work was supported by National Institutes of Health Grants R01-HL70393 (to J.C.) and R01-NS42901 (to F.T.H.) and the American Heart Association and the Whitaker Foundation (J.C.).

1. Hille, B. (2001) *Ion Channels of Excitable Membranes* (Sinauer, Sunderland, MA).
2. Yang, N. & Horn, R. (1995) *Neuron* **15,** 213–218.
3. Mannuzzu, L. M., Moronne, M. M. & Isacoff, E. Y. (1996) *Science* **271,** 213–216.
4. Seoh, S. A., Sigg, D., Papazian, D. M. & Bezanilla, F. (1996) *Neuron* **16,** 1159–1167.
5. Aggarwal, S. K. & MacKinnon, R. (1996) *Neuron* **16,** 1169–1177.
6. Liu, Y., Holmgren, M., Jurman, M. E. & Yellen, G. (1997) *Neuron* **19,** 175–184.
7. Doyle, D. A., Morais Cabral, J., Pfuetzner, R. A., Kuo, A., Gulbis, J. M., Cohen, S. L., Chait, B. T. & MacKinnon, R. (1998) *Science* **280,** 69–77.
8. Jiang, Y., Lee, A., Chen, J., Cadene, M., Chait, B. T. & MacKinnon, R. (2002) *Nature* **417,** 523–526.
9. Jiang, Y., Lee, A., Chen, J., Ruta, V., Cadene, M., Chait, B. T. & MacKinnon, R. (2003) *Nature* **423,** 33–41.
10. Jiang, Y., Ruta, V., Chen, J., Lee, A. & MacKinnon, R. (2003) *Nature* **423,** 42–48.
11. Atkinson, N. S., Robertson, G. A. & Ganetzky, B. (1991) *Science* **253,** 551–555.
12. Wallner, M., Meera, P. & Toro, L. (1996) *Proc. Natl. Acad. Sci. USA* **93,** 14922–14927.
13. Diaz, L., Meera, P., Amigo, J., Stefani, E., Alvarez, O., Toro, L. & Latorre, R. (1998) *J. Biol. Chem.* **273,** 32430–32436.
14. Cui, J. & Aldrich, R. W. (2000) *Biochemistry* **39,** 15612–15619.
15. Marty, A. (1981) *Nature* **291,** 497–500.
16. Pallotta, B. S., Magleby, K. L. & Barrett, J. N. (1981) *Nature* **293,** 471–474.
17. Golowasch, J., Kirkwood, A. & Miller, C. (1986) *J. Exp. Biol.* **124,** 5–13.
18. Shi, J. & Cui, J. (2001) *J. Gen. Physiol.* **118,** 589–606.
19. Zhang, X., Solaro, C. R. & Lingle, C. J. (2001) *J. Gen. Physiol.* **118,** 607–636.
20. Jiang, Y., Pico, A., Cadene, M., Chait, B. T. & MacKinnon, R. (2001) *Neuron* **29,** 593–601.
21. Shi, J., Krishnamoorthy, G., Yang, Y., Hu, L., Chaturvedi, N., Harilal, D., Qin, J. & Cui, J. (2002) *Nature* **418,** 876–880.
22. Xia, X. M., Zeng, X. & Lingle, C. J. (2002) *Nature* **418,** 880–884.
23. Jiang, Y., Lee, A., Chen, J., Cadene, M., Chait, B. T. & MacKinnon, R. (2002) *Nature* **417,** 515–522.
24. Butler, A., Tsunoda, S., McCobb, D. P., Wei, A. & Salkoff, L. (1993) *Science* **261,** 221–224.
25. Cui, J., Cox, D. H. & Aldrich, R. W. (1997) *J. Gen. Physiol.* **109,** 647–673.
26. Rothberg, B. S. & Magleby, K. L. (2000) *J. Gen. Physiol.* **116,** 75–100.
27. Horrigan, F. T. & Aldrich, R. W. (2002) *J. Gen. Physiol.* **120,** 267–305.
28. Monod, J., Wyman, J. & Changeux, J. P. (1965) *J. Mol. Biol.* **12,** 88–118.
29. Ledwell, J. L. & Aldrich, R. W. (1999) *J. Gen. Physiol.* **113,** 389–414.
30. Cox, D. H., Cui, J. & Aldrich, R. W. (1997) *J. Gen. Physiol.* **110,** 257–281.
31. Cox, D. H. & Aldrich, R. W. (2000) *J. Gen. Physiol.* **116,** 411–432.
32. Rothberg, B. S. & Magleby, K. L. (1999) *J. Gen. Physiol.* **114,** 93–124.
33. Schreiber, M., Wei, A., Yuan, A., Gaut, J., Saito, M. & Salkoff, L. (1998) *J. Biol. Chem.* **273,** 3509–3516.
34. Tempel, B. L., Jan, Y. N. & Jan, L. Y. (1988) *Nature* **332,** 837–839.